ICROS-SICE International Joint Conference 2009
August 18-21, 2009, Fukuoka International Congress Center, Japan

Multi-Preview Configuration Control for Predictive Behavior of Redundant Manipulator

Yusaku Nakamura[1], Tongxiao Zhang[1] and Mamoru Minami[2]

[1]Graduate school of Engineering, University of Fukui, Bunkyo3-9-1, Fukui, Japan
(Tel,Fax : +81-776-27-8527;E-mail: {yuusaku,zhangtongxiao}@rc.his.u-fukui.ac.jp)
[2]Faculty of Engineering, University of Fukui, Bunkyo 3-9-1, Fukui, Japan
(Tel,Fax: +81-776-27-8527; E-mail: minami@rc.his.u-fukui.ac.jp)

Abstract: This paper proposes a new approach named Multi-Preview Control to achieve an on-line control of trajectory tracking and obstacle avoidance for redundant manipulator. This control strategy locates between on-line local method and off-line global method (path planning). In the trajectory tracking process, the configuration of manipulator is required to possess avoidance manipulability as high as possible in real-time. Multi-Preview Control uses several future optimal configurations to control current configuration to complete task of trajectory tracking and obstacle avoidance on-line with higher avoidance manipulability and reachability. We compare Multi-Preview Control with Single-Preview Control, and verify the effectiveness and validity of Multi-Preview Control through simulations.

Keywords: Redundant manipulator, Multi-Preview Control, PA10.

1. INTRODUCTION

Over the past two decades, redundant manipulators are used for various tasks, for example, welding, sealing and grinding. These kinds of tasks require that the manipulator plan its hand onto a desired trajectory (trajectory tracking) and avoid its intermediate links, meaning all comprising links of robot except the top link with the end-effecter, from obstacles existing near the target object and also the target object itself (obstacle avoidance).

There are many researches on the motion of redundant manipulators discussing how to use the redundancy. The proposed solutions to this problem can be broadly categorized into two classes: Global Methods and Local Methods. Global Methods [1],[2] solve the collision avoidance problem by an entire path planning which is only suited for structured and static environment. Moreover, the computational cost of Global Methods is expensive and usually increases exponentially along with the number of manipulator's joints. On the other hand, Local Methods [3],[4] solve the collision problem in unstructured and dynamic environment. Local Method's system has the ability to be flexible even in surroundings with limited information. The information of the environment used in Local Method is naturally restricted to perform the tasks on-line in limited recognition time.

Our main concern in this research is whether we can connect the concepts of Local Method and Global Method by introducing a concept of Multi-Preview Control strategy. If the future information required for path planning can be available to use for Local Method, then it should be possible that the real-time configuration control in Local Method may approach the configuration behavior of Global Method. This is the research direction what we want to pursue and to make clear. Though this question has not been announced in this report, we can posit clue to approach it.

Our research pursues adaptive system using Local Method. The features of our system are shown in Fig.1

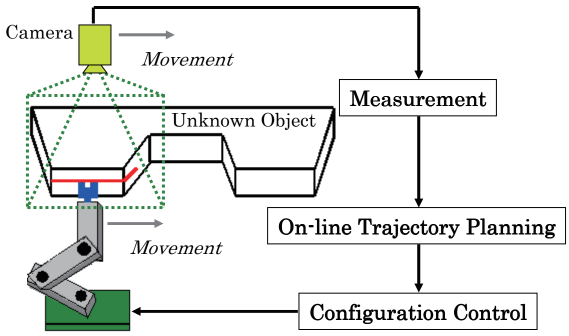

Fig. 1 Processing system for unknown object

where the camera scene area symbolizes the restricted information of environment. In Fig.1, the camera and the manipulator's hand are supposed to move synchronously to achieve on-line operation depending on the real-time restricted information. When the camera detects a new obstacle appearing suddenly in the scene, the manipulator must change its configuration immediately for avoiding it.

In our previous researches, we proposed Single-Preview Control Method [5] which uses one imaginary manipulator to explore future trajectory information to control current actual manipulator. Therefore, Single-Preview Control Method belongs to classic Local Method. Here, we propose a new method named Multi-Preview Control in this paper. Multi-Preview Control Method depends on several imaginary manipulators to acquire the more future trajectory information rather than only one, although it does not explore entirely the all trajectory like path planning. Therefore, Multi-Preview Control Method is in the position between Local Method and Global Method, the differences of these methods are explained in section 4. In addition, we will find its merits by simulations presented in section 6.

PR0002/09/0000-3117 ¥400 © 2009 SICE

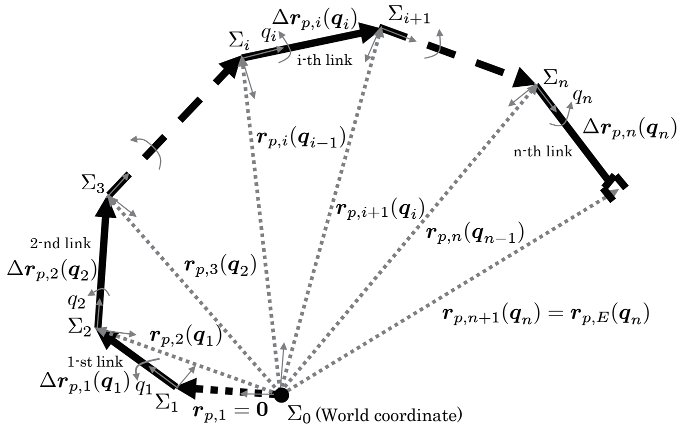

Fig. 2 Structure of n-link redundant manipulator

2. MANIPULABILITY

2.1 Redundant Manipulator's Kinematics

2.1.1 Position Space

As shown in Fig.2, Σ_0 is the world coordinate fixed in the task space, Σ_i $(i = 1, 2, \cdots, n)$ is a coordinate fixed at bottom-side of the i-th link, q_i is the rotational angle of the i-th link, n denotes the number of the manipulator's links. The position vector of top-side of the i-th link is denoted as $\boldsymbol{r}_{p,i+1}(\boldsymbol{q}_i) \in R^{m_p}$ with respect to Σ_0, and the position vector of bottom-side of the i-th link is denoted as $\boldsymbol{r}_{p,i}(\boldsymbol{q}_{i-1}) \in R^{m_p}$ with respect to Σ_0. m_p denotes the position dimension number of working space ($1 \le m_p \le 3$). $\boldsymbol{r}_{p,n+1}(\boldsymbol{q}_n) = \boldsymbol{r}_{p,E}(\boldsymbol{q}_n)$ and we simplify as $\boldsymbol{r}_{p,1} = \boldsymbol{0}$. In this paper, please notice that the all definitions will omit the left superscript "0" when they are with respect to Σ_0. When $m_p = 3$, $\boldsymbol{r}_{p,i+1}(\boldsymbol{q}_i)$ is given as a function of $\boldsymbol{q}_i$ and defined as

$$\boldsymbol{r}_{p,i+1}(\boldsymbol{q}_i) = \begin{pmatrix} x_{i+1}(\boldsymbol{q}_i) \\ y_{i+1}(\boldsymbol{q}_i) \\ z_{i+1}(\boldsymbol{q}_i) \end{pmatrix}. \tag{1}$$

In Eq.(1), $\boldsymbol{q}_i \in R^n$ and it is defined as

$$\boldsymbol{q}_i = \begin{pmatrix} q_1 \\ \vdots \\ q_i \\ 0 \\ \vdots \\ 0 \end{pmatrix}, \quad (i = 1, 2, \cdots, n). \tag{2}$$

In addition, as shown in Fig.2, $\Delta \boldsymbol{r}_{p,i}(\boldsymbol{q}_i)$ is the vector connecting bottom-side to top-side of i-th link with respect to Σ_0, so $\boldsymbol{r}_{p,i+1}(\boldsymbol{q}_i)$ can be denoted as

$$\boldsymbol{r}_{p,i+1}(\boldsymbol{q}_i) = \sum_{j=1}^{i} \Delta \boldsymbol{r}_{p,j}(\boldsymbol{q}_j). \tag{3}$$

By differentiating $\boldsymbol{r}_{p,i+1}(\boldsymbol{q}_i)$ in Eq.(3) with time, we can obtain

$$\begin{aligned} \dot{\boldsymbol{r}}_{p,i+1}(\boldsymbol{q}_i) = \frac{\partial \boldsymbol{r}_{p,i+1}(\boldsymbol{q}_i)}{\partial \boldsymbol{q}_n^T} \dot{\boldsymbol{q}}_n \\ = \frac{\partial \Delta \boldsymbol{r}_{p,1}(\boldsymbol{q}_1)}{\partial \boldsymbol{q}_n^T} \dot{\boldsymbol{q}}_n + \cdots + \frac{\partial \Delta \boldsymbol{r}_{p,i}(\boldsymbol{q}_i)}{\partial \boldsymbol{q}_n^T} \dot{\boldsymbol{q}}_n \\ = \frac{\partial \Delta \boldsymbol{r}_{p,1}(\boldsymbol{q}_1)}{\partial \boldsymbol{q}_1^T} \dot{\boldsymbol{q}}_n + \cdots + \frac{\partial \Delta \boldsymbol{r}_{p,i}(\boldsymbol{q}_i)}{\partial \boldsymbol{q}_i^T} \dot{\boldsymbol{q}}_n \\ = \boldsymbol{J}_{p,i} \dot{\boldsymbol{q}}_n, \end{aligned} \tag{4}$$

then, we can obtain the position Jacobian matrix $\boldsymbol{J}_{p,i}$ $(i = 1, 2, \cdots, n)$ in Eq.(4) as

$$\begin{aligned} \boldsymbol{J}_{p,i} &= (\underbrace{\sum_{j=1}^{i} \frac{\partial \Delta \boldsymbol{r}_{p,j}(\boldsymbol{q}_j)}{\partial q_1}, \ \cdots, \ \frac{\partial \Delta \boldsymbol{r}_{p,i}(\boldsymbol{q}_i)}{\partial q_i}}_{i}, \ \underbrace{\boldsymbol{0}}_{n-i}) \}m_p \\ &= (\tilde{\boldsymbol{j}}_{p,i,1}, \ \cdots, \ \tilde{\boldsymbol{j}}_{p,i,i}, \ \boldsymbol{0}) \\ &= (\tilde{\boldsymbol{J}}_{p,i}, \ \boldsymbol{0}). \end{aligned} \tag{5}$$

If we define $\Delta \boldsymbol{J}_{p,j}$ as

$$\begin{aligned} \Delta \boldsymbol{J}_{p,j} &= (\underbrace{\frac{\partial \Delta \boldsymbol{r}_{p,j}(\boldsymbol{q}_j)}{\partial q_1}, \ \cdots, \ \frac{\partial \Delta \boldsymbol{r}_{p,j}(\boldsymbol{q}_j)}{\partial q_j}}_{j}, \ \underbrace{\boldsymbol{0}}_{n-j}) \}m_p \\ &= (\Delta \tilde{\boldsymbol{j}}_{p,j,1}, \ \cdots, \ \Delta \tilde{\boldsymbol{j}}_{p,j,j}, \ \boldsymbol{0}) \\ &= (\Delta \tilde{\boldsymbol{J}}_{p,j}, \ \boldsymbol{0}), \end{aligned} \tag{6}$$

then, $\boldsymbol{J}_{p,i}$ $(i = 1, 2, \cdots, n)$ can be denoted by

$$\boldsymbol{J}_{p,i} = \sum_{j=1}^{i} \Delta \boldsymbol{J}_{p,j}. \tag{7}$$

2.1.2 Orientation Space

Representing the orientational vector of i-th link by $\boldsymbol{r}_{o,i}(\boldsymbol{q}_i) \in R^{m_o}$. Here, m_o denotes the orientation dimension number of working space ($1 \le m_o \le 3$). When $m_o = 3$ and $\boldsymbol{r}_{o,i}(\boldsymbol{q}_i)$ is represented by a rather common definition of "Euler angles" $(\phi_i, \theta_i, \psi_i)$, and it is given as a function of $\boldsymbol{q}_i$ as

$$\boldsymbol{r}_{o,i}(\boldsymbol{q}_i) = \begin{pmatrix} \phi_i(\boldsymbol{q}_i) \\ \theta_i(\boldsymbol{q}_i) \\ \psi_i(\boldsymbol{q}_i) \end{pmatrix}. \tag{8}$$

By differentiating $\boldsymbol{r}_{o,i}(\boldsymbol{q}_i)$ in Eq.(8) with time, we can obtain

$$\dot{\boldsymbol{r}}_{o,i}(\boldsymbol{q}_i) = \frac{\partial \boldsymbol{r}_{o,i}(\boldsymbol{q}_i)}{\partial \boldsymbol{q}_n^T} \dot{\boldsymbol{q}}_n. \tag{9}$$

Providing z-axis of Σ_i represents rotational axis and it is denoted by $\boldsymbol{z}_i$, the angular velocity vector $\boldsymbol{\omega}_i$ is

$$\boldsymbol{\omega}_i = \sum_{j=1}^{i} \boldsymbol{z}_j \dot{q}_j. \tag{10}$$

And the relation between $\boldsymbol{\omega}_i$ and $\dot{\boldsymbol{r}}_{o,i}(\boldsymbol{q}_i)$ is

$$\begin{aligned} \boldsymbol{\omega}_i &= \begin{pmatrix} 0 & -sin\phi_i & cos\phi_i sin\theta_i \\ 0 & cos\phi_i & sin\phi_i sin\theta_i \\ 1 & 0 & cos\theta_i \end{pmatrix} \dot{\boldsymbol{r}}_{o,i}(\boldsymbol{q}_i) \\ &= \begin{pmatrix} 0 & -sin\phi_i & cos\phi_i sin\theta_i \\ 0 & cos\phi_i & sin\phi_i sin\theta_i \\ 1 & 0 & cos\theta_i \end{pmatrix} \frac{\partial \boldsymbol{r}_{o,i}(\boldsymbol{q}_i)}{\partial \boldsymbol{q}_n^T} \dot{\boldsymbol{q}}_n \\ &= \boldsymbol{J}_{o,i} \dot{\boldsymbol{q}}_n. \end{aligned} \tag{11}$$

From Eq.(10) and Eq.(11), $\boldsymbol{J}_{o,i}$ is denoted as

$$\begin{aligned}\boldsymbol{J}_{o,i} &= (\underbrace{\boldsymbol{z}_1,\cdots,\boldsymbol{z}_i}_{i},\underbrace{\boldsymbol{0}}_{n-i})\}m_o \\ &= (\tilde{\boldsymbol{J}}_{o,i},\ \boldsymbol{0}). \quad (12)\end{aligned}$$

Being similar with the description of Eq.(7), $\boldsymbol{J}_{o,i}$ ($i = 1,2,\cdots,n$) can be denoted as

$$\boldsymbol{J}_{o,i} = \sum_{j=1}^{i}\Delta\boldsymbol{J}_{o,j}. \quad (13)$$

2.1.3 Conbined Position and Orientation Spaces

According to above analyses in position space ($m_p = 3$) and orientation space ($m_o = 3$) respectively, in the maximum space of $m = m_p + m_o = 6$, we can define

$$\boldsymbol{p}_i(\boldsymbol{q}_i) = \begin{pmatrix} \boldsymbol{r}_{p,i+1}(\boldsymbol{q}_i) \\ \boldsymbol{r}_{o,i}(\boldsymbol{q}_i) \end{pmatrix} \quad (14)$$

and

$$\begin{aligned}\underline{\dot{\boldsymbol{r}}}_i(\boldsymbol{q}_i) &= \begin{pmatrix} \dot{\boldsymbol{r}}_{p,i+1}(\boldsymbol{q}_i) \\ \boldsymbol{\omega}_i \end{pmatrix} \\ &= \begin{pmatrix} \dot{x}_{i+1}(\boldsymbol{q}_i) \\ \dot{y}_{i+1}(\boldsymbol{q}_i) \\ \dot{z}_{i+1}(\boldsymbol{q}_i) \\ \omega_{x,i} \\ \omega_{y,i} \\ \omega_{z,i} \end{pmatrix} \\ &= \begin{pmatrix} \boldsymbol{J}_{p,i} \\ \boldsymbol{J}_{o,i} \end{pmatrix}\dot{\boldsymbol{q}}_n \\ &= \underline{\boldsymbol{J}}_i\dot{\boldsymbol{q}}_n. \quad (15)\end{aligned}$$

In this way, according to $\underline{\dot{\boldsymbol{r}}}_i(\boldsymbol{q}_i)$, we can define

$$\begin{aligned}\dot{\boldsymbol{r}}_i(\boldsymbol{q}_i) &= \underline{\boldsymbol{U}}_m\underline{\dot{\boldsymbol{r}}}_i(\boldsymbol{q}_i) \\ &= \underline{\boldsymbol{U}}_m\underline{\boldsymbol{J}}_i\dot{\boldsymbol{q}}_n \\ &= \boldsymbol{J}_i\dot{\boldsymbol{q}}_n. \quad (16)\end{aligned}$$

In Eq.(16), $\underline{\boldsymbol{U}}_m$ is an $m\times 6$ matrix to select hand's task space. For example, when the hand's task space is given by $m = 3$ such as $\dot{\boldsymbol{r}}_i(\boldsymbol{q}_i) = [\dot{x}_{i+1}(\boldsymbol{q}_i), \dot{y}_{i+1}(\boldsymbol{q}_i), \omega_{z,i})]^T$, $\underline{\boldsymbol{U}}_m$ is a 3×6 matrix as

$$\underline{\boldsymbol{U}}_m = \begin{pmatrix} 1 & 0 & 0 & 0 & 0 & 0 \\ 0 & 1 & 0 & 0 & 0 & 0 \\ 0 & 0 & 0 & 0 & 0 & 1 \end{pmatrix}. \quad (17)$$

In addition, being similar with the descriptions of Eq.(7) and Eq.(13), we can define

$$\begin{aligned}\boldsymbol{J}_i &= \sum_{j=1}^{i}\Delta\boldsymbol{J}_j \\ &= (\tilde{\boldsymbol{J}}_i,\ \boldsymbol{0}) \quad (18)\end{aligned}$$

and

$$\Delta\boldsymbol{J}_j = \underline{\boldsymbol{U}}_m\begin{pmatrix} \Delta\boldsymbol{J}_{p,j} \\ \Delta\boldsymbol{J}_{o,j} \end{pmatrix}. \quad (19)$$

In this paper, the discussion of $rank({}^1\boldsymbol{M}_i)$ will not be affected whatever joint of the manipulator to be analyzed.

2.2 Manipulability Ellipsoid

Considering a set of tip velocities $\dot{\boldsymbol{r}}_i$ of all links being realizable by a set of joint angle velocities $\dot{\boldsymbol{q}}_n$ that satisfies an Euclidean norm condition, that is, $\|\dot{\boldsymbol{q}}_n\| = (\dot{q}_1^2 + \dot{q}_2^2 + \cdots + \dot{q}_n^2)^{1/2} \le 1$, then the each tip velocity shapes an ellipsoid in range space of $\boldsymbol{J}_i$. These ellipsoids have been known as "manipulability ellipsoid"[8], [9], which are described as

$$\dot{\boldsymbol{r}}_i^T(\boldsymbol{J}_i^+)^T\boldsymbol{J}_i^+\dot{\boldsymbol{r}}_i \le 1, \quad \dot{\boldsymbol{r}}_i \in R(\boldsymbol{J}_i). \quad (20)$$

In Eq.(20), $\boldsymbol{J}_i^+$ is pseudo-inverse of $\boldsymbol{J}_i$, and $R(\boldsymbol{J}_i)$ represents range space of $\boldsymbol{J}_i$.

3. AVOIDANCE MANIPULABILITY SHAPE INDEX WITH POTENTIAL

We proposed Avoidance Manipulability Ellipsoid and Avoidance Manipulability Shape Index (AMSI) in [6], and Avoidance Manipulability Shape Index with Potential (AMSIP) in [5]. Avoidance Manipulability Ellipsoid is applied from Manipulability Ellipsoid proposed by Prof. Yoshikawa in [7]. We will elucidate them briefly in this section.

Referring to Eq.(16), when desired hand velocity $\dot{\boldsymbol{r}}_{nd}$ is given, $\dot{\boldsymbol{q}}_n$ is solved as

$$\dot{\boldsymbol{q}}_n = \boldsymbol{J}_n^+\dot{\boldsymbol{r}}_{nd} + (\boldsymbol{I}_n - \boldsymbol{J}_n^+\boldsymbol{J}_n)\,{}^1\boldsymbol{l}, \quad (21)$$

where $\boldsymbol{J}_n^+$ is the pseudo-inverse of Jacobean Matrix $\boldsymbol{J}_n$ and $\boldsymbol{I}_n$ is a $n\times n$ unit matrix. In addition, ${}^1\boldsymbol{l}$ is an arbitrary vector. Trajectory tracking of the hand and collision avoidance can executed simultaneously through this vector ${}^1\boldsymbol{l}$. Here, control variable ${}^1\boldsymbol{l}$ is determined so as to make actual manipulator's shape at current time $\boldsymbol{q}(t)$ close to future optimal shape by referring to the future optimal shapes of imaginary manipulators. The relation of the desired angular velocity of the i-th link ${}^1\dot{\boldsymbol{r}}_{id}$ and $\dot{\boldsymbol{r}}_{nd}$ is shown in Eq.(22) by substituting Eq.(21) to Eq.(16).

$${}^1\dot{\boldsymbol{r}}_{id} = \boldsymbol{J}_i\boldsymbol{J}_n^+\dot{\boldsymbol{r}}_{nd} + \boldsymbol{J}_i(\boldsymbol{I}_n - \boldsymbol{J}_n^+\boldsymbol{J}_n)\,{}^1\boldsymbol{l} \quad (22)$$

Here we define two variables shown in Eq.(23) and Eq.(24).

$$\Delta{}^1\dot{\boldsymbol{r}}_{id} \stackrel{\triangle}{=} {}^1\dot{\boldsymbol{r}}_{id} - \boldsymbol{J}_i\boldsymbol{J}_n^+\dot{\boldsymbol{r}}_{nd}, \quad (23)$$

$${}^1\boldsymbol{M}_i \stackrel{\triangle}{=} \boldsymbol{J}_i(\boldsymbol{I}_n - \boldsymbol{J}_n^+\boldsymbol{J}_n). \quad (24)$$

According to Eq.(22),Eq.(23) and Eq.(24), $\Delta{}^1\dot{\boldsymbol{r}}_{id}$ can be rewritten as

$$\Delta{}^1\dot{\boldsymbol{r}}_{id} = {}^1\boldsymbol{M}_i\,{}^1\boldsymbol{l}. \quad (25)$$

In Eq.(25), $\Delta{}^1\dot{\boldsymbol{r}}_{id}$ is called the first avoidance velocity and ${}^1\boldsymbol{M}_i$ is a $m\times n$ matrix called the first avoidance matrix.

Next, we will represent the avoidance manipulability measure and the Avoidance Manipulability Ellipsoid. Providing that ${}^1\boldsymbol{l}$ is restricted as $\|{}^1\boldsymbol{l}\| \le 1$, then the extent where $\Delta{}^1\dot{\boldsymbol{r}}_{id}$ can move is denoted as

$$\Delta{}^1\dot{\boldsymbol{r}}_{id}^T({}^1\boldsymbol{M}_i^+)^T\,{}^1\boldsymbol{M}_i^+\Delta{}^1\dot{\boldsymbol{r}}_{id} \le 1. \quad (26)$$

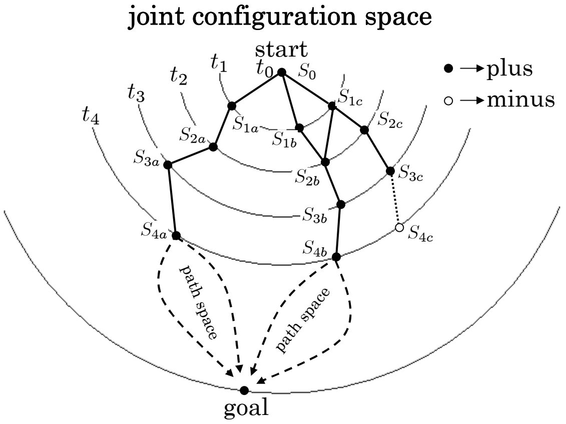

Fig. 3 The concept of single-preview and multi-preview

If $rank(^1\boldsymbol{M}_i) = m$, the ellipsoid represented by Eq.(26) is named the first complete avoidance manipulability ellipsoid. If $rank(^1\boldsymbol{M}_i) = p < m$, the ellipsoid is named as the first partial avoidance manipulability ellipsoid.

The volume of each Avoidance Manipulability Ellipsoid indicates mobility of each link (shape-changeability). The larger total volume indicates the higher whole avoidance manipulability. We evaluated total volume as Avoidance Manipulability Shape Index (AMSI). Then we proposed Avoidance Manipulability Shape Index with Potential (AMSIP) which considers AMSI and the distance between the manipulator and target object. And we verified the superiority of AMSIP through the simulation in [5].

4. CONCEPT

Single-Preview Control and Multi-Preview Control use the future trajectory information obtained by the camera to control actual manipulator. Basically, these methods make the actual manipulator close to the future manipulator (imaginary manipulator) whose configuration possesses the higher avoidance manipulability and ensures non-collision. Single-Preview Control uses an imaginary manipulator with very limited information and Multi-Preview Control uses several imaginary manipulators with more information.

Fig.3 describes the effectiveness of multiple preview control, where the times defined by t_0, t_1, t_2, t_3 and t_4 respectively. And "$\bullet$" indicates several local optimal configurations at each future time whose evaluation values ^1S presented in [5] are plus and are denoted here by S_{1a}, S_{1b}, S_{1c} ($S_{1a} < S_{1b} < S_{1c}$) at $t = t_1$, and S_{2a}, S_{2b}, S_{2c} ($S_{2a} < S_{2b} < S_{2c}$) at $t = t_2$, and S_{3a}, S_{3b}, S_{3c} ($S_{3a} < S_{3b} < S_{3c}$) at $t = t_3$ and S_{4b}, S_{4c} ($S_{4b} < S_{4c}$) at $t = t_4$. The value S evaluates superiority of the configuration and safety concerning collision with the working object, and $S < 0$ means collision. The manipulator stays at initial configuration when time $t = t_0$. If we do not use preview control method, we almost can not know the future information, so control of the current manipulator's configuration will be blind without any reference. If we use single preview depending on only one future optimal configuration at one future time, then the configuration will be controlled to S_{1c} at time $t = t_1$, to S_{2c} at time $t = t_2$ and to S_{3c} at time $t = t_3$. Shall we provide that the value of S_{4a} has negative value represented by "$\circ$" meaning future possible configuration from S_{3c} can not avoid collision with surroundings or target object. The configuration of redundant manipulator corresponding to S_{3c} at time $t = t_3$ is trapped in hardship because the future information at only one future time is very local. The real-time motion will have to be stopped at time $t = t_3$ for safety. However, if we expand the future information by selecting three future optimal configurations at three future times, which is Multi-Preview. The configuration will be controlled to S_{1c} at time $t = t_0$ by the future optimal reachable sequences $S_0 \to S_{1c} \to S_{2c} \to S_{3c}$ estimated from $S_{ij} (i = 1, 2, 3; j = a, b, c)$, where the other possible sequences $S_0 \to S_{1a} \to S_{2a} \to S_{3a}$, $S_0 \to S_{1b} \to S_{2b} \to S_{3b}$ and $S_0 \to S_{1c} \to S_{2b} \to S_{3b}$ are inferior selection. Then, the possible future sequences at time t_1 are restricted to $S_{1c} \to S_{2b} \to S_{3b} \to S_{4c}$ and $S_{1c} \to S_{2c} \to S_{3c} \to S_{4a}$, and then both are evaluated. Then multi-preview controller can judge and exclude the collision configuration S_{4a}, then it will choose the future optimal reachable sequences $S_{1c} \to S_{2b} \to S_{3b} \to S_{4c}$. By repeating such evaluation of future configuration sequences and possible route changing, multi-preview control system will possibly avoid dangerous sequences connecting to clashing in the future and can widen out the reachable possibility from current configuration to goal configuration.

According to above discussion, we can conceptually think that Multi-Preview Control can improve the limitation of Single-Preview Control.

5. MULTI PREVIEW CONTROL

Multi-Preview Control System is shown in Fig.4 which is a configuration control method to change current manipulator's shape satisfying non-collision requirement by referring to the future configurations based on an on-line measurement.

It consists of an on-line measurement block, a path planning block, a redundancy control block and redundant manipulator. On the assumption that current time is represented by t, and the future times are defined as $t_i^* = t + i\tilde{t}$, $(i \in [1, p])$ where $\tilde{t}$ denotes preview time and i is the number of future times. A measurement block detects a desirable hand position $\boldsymbol{r}_d(t_i^*)$ on the surface of the target object at time t_i^*, which is reasonably assumed to be possible to detect the future information only in the detected camera image in Fig.1. Firstly, potential space based on the detected shape of the target object is created around it at the path planning block. Then the path planning block outputs the optimal shape $\tilde{\boldsymbol{q}}_d(t_i^*)$ corresponding to the maximum ^1S presented in [5] at the future time t_i^* (imaginary manipulator) by 1-Step GA. The control block outputs desired joint angular velocity $\dot{\boldsymbol{q}}_d(t)$ that makes actual manipulator's shape at current time $\boldsymbol{q}(t)$

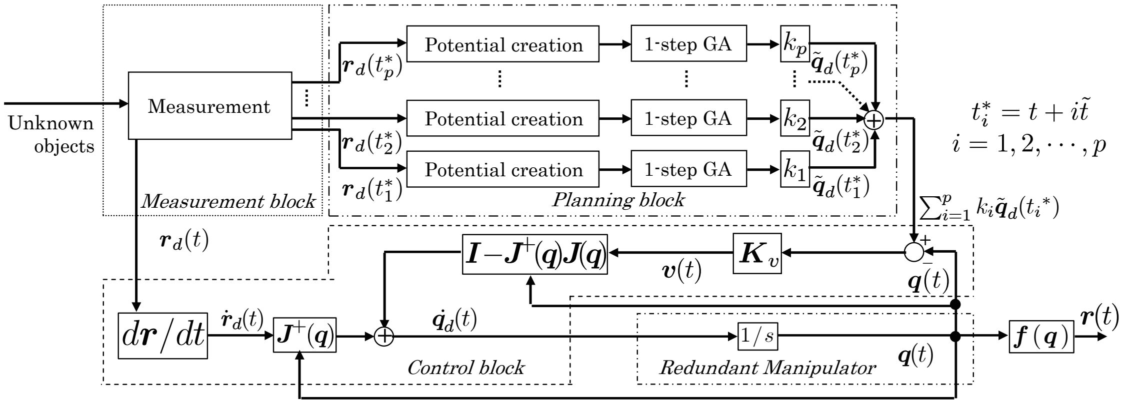

Fig. 4 Multi-Preview control system

close to the optimal shape in the future by referring to $\sum_{i=1}^{p} \tilde{q}_d(t_i^*)$.

An equation which realizes this control system is named as Preview Control Equation and expressed as follows

$$\begin{aligned} \dot{q}_d &= J_n^+ \dot{r}_{nd} \\ &+ (I_n - J_n^+ J_n) K_v (\sum_{i=1}^{p} \tilde{q}_d(t_i^*) - q(t)). \end{aligned} \quad (27)$$

where $n \times 1$ matrix $\sum_{i=1}^{p} \tilde{q}_d(t_i^*) - q(t)$ is defined as

$$\sum_{i=1}^{p} \tilde{q}_d(t_i^*) - q(t) = \begin{bmatrix} \sum_{i=1}^{p} \tilde{q}_{1d}(t_i^*) - q_1(t) \\ \vdots \\ \sum_{i=1}^{p} \tilde{q}_{jd}(t_i^*) - q_j(t) \\ 0 \\ \vdots \\ 0 \end{bmatrix}, \quad (28)$$

when redundant degrees j remains and the redundancy is used for the joints from 1 to j.

The transition of AMSIP and the manipulator's shape using Multi-Preview Control System is shown in Fig.5. According to Fig.5, we can find that the manipulator can always keep higher AMSIP value by using Multi-Preview Control. And the AMSIP value obtained by this system moves from one higher peak to another higher peak as time in multi peak AMSIP distributions. This verifies the validity of Multi-Preview Control in 2-dimension by 4-link planar manipulator.

6. SIMULATIONS

We examine the same simulations with different controller, such as Single-Preview Control and Multi-Preview Control, for verifying the validity of the latter. An top view of the target object is shown in Fig.6 and corresponding potential spaces are set in Fig.7. In this simulation, we use exact model of the 7-link manipulator

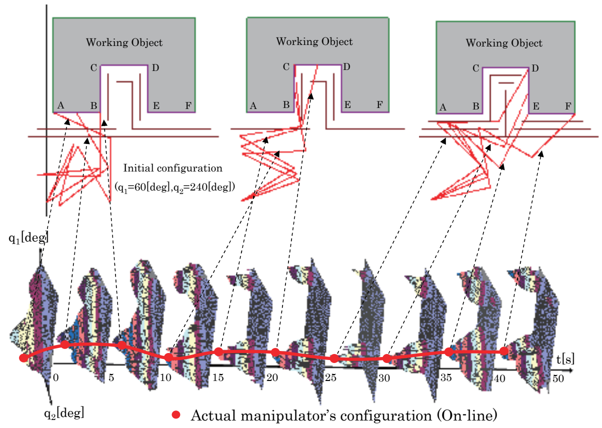

Fig. 5 Actual manipulator's configurations in whole tracking process based on multi-preview control

named PA10 (Mitsubishi Heavy Industries, Ltd.) and a desired trajectory r_d is defined as follows

$$r_d = \begin{cases} r_{dx} = -0.8[m] \\ r_{dy} = -0.5 + 0.05t[m] \\ r_{dz} = 0.6[m] \end{cases} . \quad (29)$$

This simulation will end at 18[s].

The working space dimension of the manipulator's hand is set at 5, where position dimension is 3 (x, y, z) and posture dimension is 2 (ω_y, ω_z). Then the manipulator has 2 redundant DoF because PA10 has 7 DoF. And we gave this 2 redundant DoF to 1-st joint, q_1, and 2-nd joint, q_2. Resolving inverse kinematics of PA10, we can determine from q_3 to q_7.

In the simulation using Single-Preview Control, we set the one future time as $t^* = t + 3[s]$. In the simulation using Multi-Preview Control, we set the three future times as $t^* = t + 3i[s], i \in [1, 3]$. The simulation results of Single-Preview Control are shown in Fig.8 and Fig.9, and the simulation results of Multi-Preview Control are shown in Fig.10 and Fig.11. Fig.8 and Fig.10 indicate a configuration transition of PA10, Fig.9 and Fig.11 indicate a distance between PA10 and the working object. In this paper, we put this distance in a potential space which is set around the working object and has negative value,

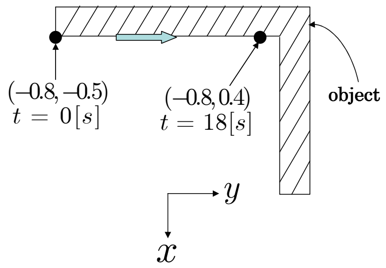

Fig. 6 Top view of target object

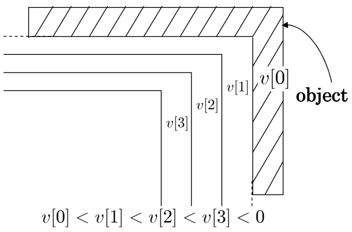

Fig. 7 Potential spaces

Fig.9 and Fig.11 show the potential value. If the potential value falls below -1000 then the manipulator collides against the working object. The manipulator in Single-Preview Control simulation is closing to the working object as time according to Fig.8 and Fig.9. On the other hand, the manipulator in Multi-Preview Control simulation is keeping the desired distance between its links and the working object according to Fig.10 and Fig.11 since the potential value [5] is not far than the value of Single-Preview given by Fig.9.

AMSIP distributions are shown from Fig.12 to Fig.18 with the interval of 3 seconds. A high AMSIP value means that the manipulator has higher shape-changeability and keeps the distance between its links and the working obstacle. In these figures, a white cross indicates an transient AMSIP value of the manipulator at the current time when using Multi-Preview Controller and a white circle indicates an AMSIP value of the manipulator when using Single-Preview Controller. Please notice that the both AMSIP values are same when time $t = 0$[s] because of the initial configuration. According to these figures, we find the former is always keeping a very higher value than latter.

We think above differences have roots in the number of imaginary manipulators which are used to control the actual manipulator as reference. In other words, Multi-Preview Control can reduce the possibility of collision exploiting future information by using imaginary manipulators.

7. CONCLUSION

In this paper, we propose and compare two methods: Single-Preview Control and Multi-Preview Control. Single-Preview Control belongs to classic Local Method and Multi-Preview Control is between Global Method and Local Method. As a results of simulation,

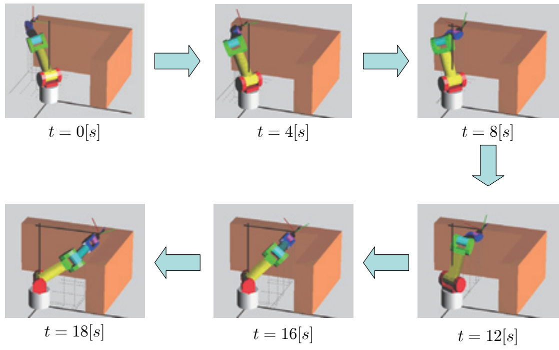

Fig. 8 Process of single-preview control

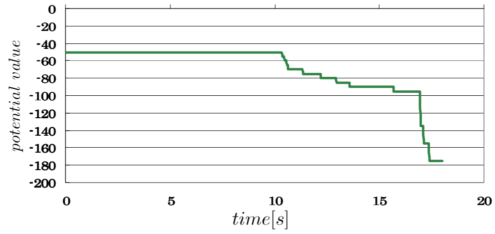

Fig. 9 Distance in single-preview control

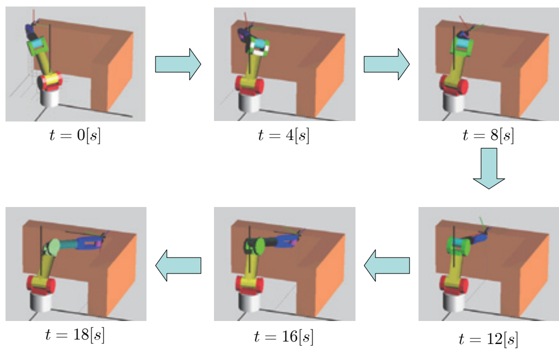

Fig. 10 Process of multi-preview control

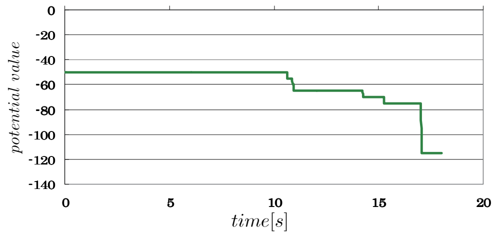

Fig. 11 Distance in multi-preview control

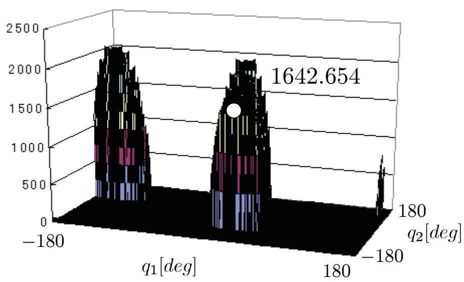

Fig. 12 AMSIP distribution at $t = 0$[s]

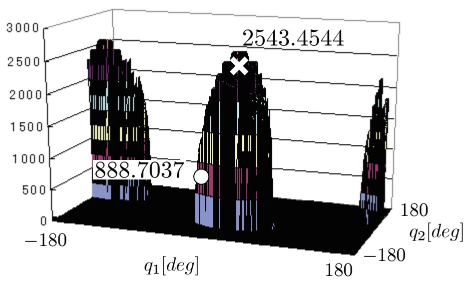

Fig. 13 AMSIP distribution at $t = 3$[s]

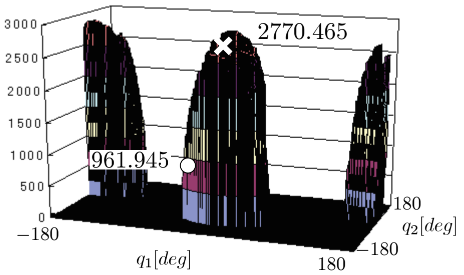

Fig. 14 AMSIP distribution at $t = 6$[s]

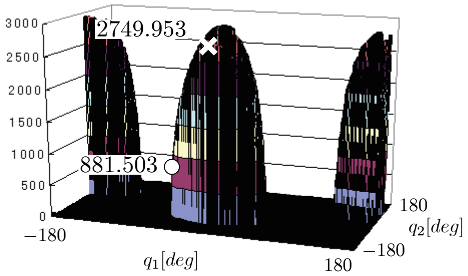

Fig. 15 AMSIP distribution at $t = 9$[s]

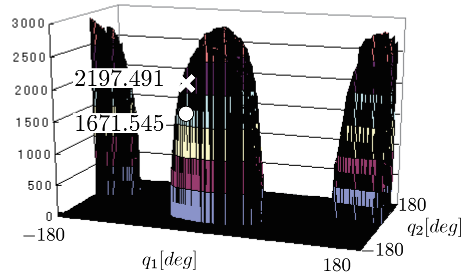

Fig. 16 AMSIP distribution at $t = 12$[s]

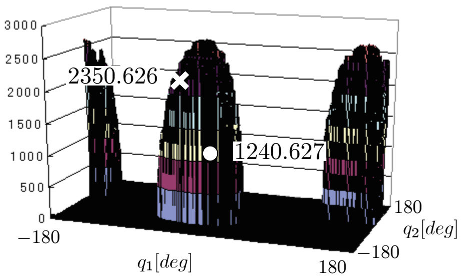

Fig. 17 AMSIP distribution at $t = 15$[s]

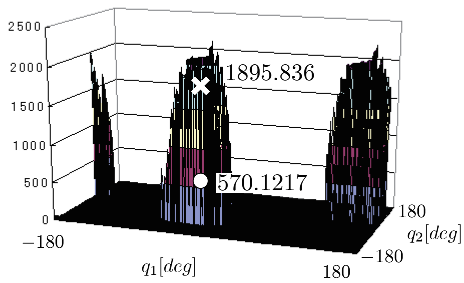

Fig. 18 AMSIP distribution at $t = 18$[s]

we show Multi-Preview Control is superior to Single-Preview Control and it has merits of Global Method and Local Method.

REFERENCES

[1] Rodrigo S. Jamisola, Jr. Anthony A. Maciejewski, Rodney G. Roberts "Failure-Tolerant Path Planning for Kinematically Redundant Manipulators Anticipating Locked-Joint Failures", IEEE Transactions on Robotics, Vol.22, No.4, 2006, pp.603-612.

[2] Juan Manuel Ahuactzin, Kamal K. Gupta "The Kinematic Roadmap: A Motion Planning Based Global Approach for Inverse Kinematics of Redundant Robots", IEEE Transactions on Robotics and Automation, Vol.15, No.4, 1999, pp.653-669.

[3] Leon Zlajpah, Bojan Nemec, "Kinematic Control Algorithms for On-line Obstacle Avoidance for Redundant Manipulator", International Conference on Intelligent Robots and Systems, 2002, pp.1898-1903.

[4] Homayoun Seraji, Bruce Bon, "Real-Time Collsion Avoidance for Position-Controlled Manipulators", IEEE Transactions on Robotics and Automation, Vol.15, No.4, 1999, pp.670-677.

[5] Keiji Ikeda, Hiroshi Tanaka, Tong-xiao Zhang, Mamoru Minami, Yasushi Mae, "On-line Optimization of Avoidance Ability for Redundant Manipulator", International Conference on Intelligent Robots and Systems, Beijing, 2006, pp.592-597.

[6] Hiroshi Tanaka, Mamoru Minami and Yasushi Mae, "Trajectory Tracking of Redundant Manipulators Based on Avoidance Manipulability Shape Index ", International Conference on Intelligent Robots and Systems, Edmonton, 2005, pp.1892-1897.

[7] Tsuneo Yoshikawa, "Foundations of Robot Control ", CORONA PUBLISHING CO., LTD.,1988

[8] Tsuneo Yoshikawa, "Measure of Manipulability for Robot Manipulators", (in Japanese) *Journal of the Robotics Society of Japan*, Vol.2, No.1, pp.63-71, 1984.

[9] Tsuneo Yoshikawa, "Manipulability of Robot Mechanisms", *The International Journal of Robotics Research*, Vol.4, No.2, pp.3-9, 1985.